Brain Pathology ISSN 1015-6305

RESEARCH ARTICLE

Myeloid-Derived Suppressor Cells Limit the Inflammation by Promoting T Lymphocyte Apoptosis in the Spinal Cord of a Murine Model of Multiple Sclerosis

Verónica Moliné-Velázquez[1]; Henar Cuervo[2]; Virginia Vila-del Sol[1]; María Cristina Ortega[1]; Diego Clemente[1]*; Fernando de Castro[1]*

[1] Grupo de Neurobiología del Desarrollo-GNDe, Hospital Nacional de Parapléjicos, Finca "La Peraleda" s/n, Toledo, Spain.
[2] Centro de Biología Molecular "Severo Ochoa", CSIC–Universidad Autónoma de Madrid, Cantoblanco, Madrid, Spain.

Keywords
apoptosis, demyelination, EAE, immunomodulation, lymphocyte, macrophage, remyelination.

Corresponding author:
Diego Clemente, PhD, Grupo de Neurobiología del Desarrollo-GNDe, Hospital Nacional de Parapléjicos, Finca "La Peraleda" s/n, E-45071 Toledo, Spain (E-mail: *dclemente@sescam.jccm.es*)

Received 26 January 2011; accepted 29 March 2011.

* These authors contributed equally to this work.

doi:10.1111/j.1750-3639.2011.00495.x

Abstract

Multiple Sclerosis (MS) is a demyelinating/inflammatory disease of the central nervous system. Relapsing-remitting MS is characterized by a relapsing phase with clinical symptoms and the production of inflammatory cell infiltrates, and a period of remission during which patients recover partially. Myeloid-derived suppressor cells (MDSCs) are immature cells capable of suppressing the inflammatory response through Arginase-I (Arg-I) activity, among other mechanisms. Here, we have identified Arg-I$^+$-MDSCs in the spinal cord during experimental autoimmune encephalomyelitis (EAE), cells that were largely restricted to the demyelinating plaque and that always exhibited the characteristic MDSC surface markers Arg-I/CD11b/Gr-1/M-CSF1R. The presence and density of Arg-I$^+$-cells, and the proportion of apoptotic but not proliferative T cells, were correlated with the EAE time course: peaked in parallel with the clinical score, decreased significantly during the remitting phase and completely disappeared during the chronic phase. Spinal cord-isolated MDSCs of EAE animals augmented the cell death when co-cultured with stimulated control splenic CD3 T cells. These data point to an important role for MDSCs in limiting inflammatory damage in MS, favoring the relative recovery in the remitting phase of the disease. Thus, the MDSC population should be considered as a potential therapeutic target to accelerate the recovery of MS patients.

INTRODUCTION

Multiple sclerosis (MS) is a chronic autoimmune demyelinating disease characterized by a coordinated inflammatory attack on the myelin sheath in the central nervous system (CNS), thereby damaging the underlying axon (13). There are four main clinical forms of MS, the most common of which is the relapsing-remitting (RR) form (85% of MS patients, at least in its initial stages) (13). The RR-MS variant is characterized by acute relapses of neurological deficits separated by periods of remission during which disease progression is halted. In order to develop new treatment strategies for chronic inflammatory diseases, it is not only important to characterize the mechanisms that trigger immune responses, but also to fully understand the factors that mediate these reactions. Indeed, awareness of the downstream effector cells that regulate inflammatory responses may aid the discovery of new and/or improved approaches for disease intervention.

Experimental autoimmune encephalomyelitis (EAE) is an autoimmune inflammatory disease that has been extensively used as an animal model of MS (22). EAE is initiated through the peripheral activation and proliferation of myelin-specific CD4 T cells, which then migrate to the CNS (24). Once inside, microglia and astrocytes are activated, and a large number of macrophages and neutrophils are recruited from the circulating blood, which results in CNS inflammation (4, 45, 51). Each phase of EAE is regulated by a distinct group of cytokines. During the onset and relapsing period, Th1 cytokines are thought to mediate the severity of the disease (24), although this may not always be the case. Indeed, mice lacking some of the main Th1 cytokines (IFN-γ, IL-12 or TNF-α) experience similar or more severe forms of EAE (16, 17, 33). In contrast, Th2 cytokines like IL-4, IL-10 and IL-13 are generally associated with EAE recovery and the induction of tolerance (3, 5). A Th17 response was recently described (31, 35) and a role for Th17 cells was revealed in the first stages after immunization prior to the onset of clinical EAE symptoms (37, 42).

Nevertheless, there is a dearth of data regarding the cell populations that affect and, in turn, are affected by the changes in cytokine composition in EAE (50), most of which relate to regulatory T cells (12, 25, 46). In recent years, a population of myeloid cells suppressing immune responses against tumors, traumatic stress, sepsis and infections (14, 23, 34, 48) has also been described participating in demyelinating animal models (6, 44, 55). These myeloid-derived

© 2011 The Authors; Brain Pathology © 2011 International Society of Neuropathology

suppressor cells (MDSCs) are a heterogeneous population that includes immature macrophages, granulocytes, dendritic cells and other myeloid cells (7, 20, 53). MDSCs have been proposed to suppress the immune response through different mechanisms: down-regulation of CD3ζ-chain expression (and the subsequent inhibition of T cell proliferation), inhibition of CD8 T cell-mediated cytotoxicity and induction of T cell apoptosis (2, 19, 27, 40). These MDSCs mainly exert their functions through iNOS and/or Arginase-I (Arg-I) activity (9, 27), a hydrolytic enzyme responsible for converting arginine to ornithine and urea (29). In mammals, Arg-I is primarily expressed in the liver and it is a critical element in the urea cycle (29). *Arg-I* is the gene that is most strongly up-regulated in the spinal cord during EAE (11, 52), and it is expressed in immature myeloid cells (isolated from EAE mouse spleen) treated with IL-4 *in vitro* (55). However, no relevant data exist regarding the distribution of these Arg-I$^+$-suppressor cells in the CNS.

In this study, we have analyzed the Arg-I expression pattern during EAE and we describe its expression by MDSCs, although only during periods in which the immune response occurs. Suppressive monocytes isolated from the spleens of EAE mice exerted their immunosuppressive actions *in vitro* by inhibiting T cell proliferation and the induction of massive cell death (55). To our knowledge, this is the first study to describe the specific relationship between Arg-I$^+$-MDSCs from the spinal cord of immunized animals (EAE) and T cell apoptosis using both *in vivo* and *in vitro* approaches. Together, our results suggest that the modulation of MDSCs in demyelinating diseases, including MS, may constitute an effective therapeutic tool to down-regulate the immune response, thereby aiding patient recovery.

MATERIALS AND METHODS

Induction of EAE

Six- to 8-week-old female C57/BL6 mice were immunized subcutaneously with 200 μg of $MOG_{35–55}$ peptide (kindly provided by Dr A. Silva, *Centro de Investigaciones Biológicas*, Madrid, Spain) in Incomplete Freund Adjuvant (v/v, Sigma, St Louis, MO, USA) containing 4 μg of *Mycobacterium tuberculosis* (H37RA, Difco, Franklin Lakes, NJ, USA). Sham-operated animals received phosphate-buffered saline (PBS) instead of the MOG peptide. Both immunized and sham mice were intravenously administered pertussis toxin (250 ng, Sigma) by injection in the tail vein at the time of immunization and 48 h later. All animal manipulations were carried out in accordance with Spanish (RD223/88) and European (86/609/ECC) regulations, and they were approved by the Animal Review Board (registered as SAPA001) at our Institution. During EAE, the clinical symptoms of MOG-immunized, sham and control animals were scored daily by three independent blind observers as follows: 0, no detectable signs of EAE; 1, tail paralyzed; 2, unilateral partial hind-limb paralysis; 3, complete bilateral hind-limb paralysis; 4, total paralysis of forelimb and hind-limb; and 5, death.

Tissue sampling

For histology, four mice were sacrificed at each of the stages analyzed during the EAE time course: 15, 25, 35 and 63 days post-immunization (dpi). The clinical score variability at each time-point was as follows: 15 dpi (2.25–3.5), 25 dpi (1.5–2.5) and 35/63 dpi (1.5–2.0). All animals were perfused transcardially with 4% paraformaldehyde in 0.1 M PB (pH 7.4) and the spinal cords were dissected out and post-fixed in the same fixative for 4 h at room temperature (RT). After immersion in 30% (w/v) sucrose in PB for 12 h, coronal sections (20 μm thick) were obtained on a cryostat (Leica, Nussloch, Germany) and they were thaw-mounted on Superfrost® Plus slides.

Eriochrome cyanine for myelin staining

The sections were dried for 2 h at RT, and for 2 h at 37°C in a slide warmer. The slides were then placed in fresh acetone for 5 min at RT, and air-dried for 30 min. The sections were stained in 0.2% eriochrome cyanine (EC) solution for 30 min and differentiated in 5% iron alum and in borax-ferricyanide for 15 and 20 min, respectively, with brief rinses under running water between each step.

Immunohistochemistry

After several rinses with PB, the sections were pre-treated for 20 min with PB containing 3% H_2O_2, 10% methanol (or methanol alone for immunofluorescence experiments). The sections were pre-incubated for 1 h at RT in incubation buffer: 5% normal serum (Vector, Burlingame, CA, USA) and 0.2% Triton X-100 (Merck, Darmstadt, Germany) diluted in PBS. Immunohistochemistry was performed by incubating sections overnight at 4°C with the primary

Table 1. Antibodies employed for the inmunohistochemical analysis in this study.

Antibody	Target	Dilution	Class	Manufacturer
Arg-I	Arginase-I enzyme	1:25	Goat polyclonal	SCBT
CD4	CD4 T lymphocytes	1:25	Rat monoclonal	eBioscience
CD8	CD8 T lymphocytes	1:25	Rat monoclonal	eBioscience
CD11b	Microglia/macrophages	1:250	Rat monoclonal	AbD, Serotec
CD115	M-CSFR1	15 μg/mL	Rabbit polyclonal	Lifespan
Gr-1	Granulocytes	1:250	Rat polyclonal	BD
Ly6B.2	Polimorphonuclear cells	1:100	Rat monoclonal	AbD, Serotec
MBP	Myelin Basic Protein	1:25	Rat monoclonal	Abcam
Tomato Lectin	Microglia/macrophages	15 μg/mL	Biotinilated	Sigma Aldrich
TUNEL	Apoptotic cells			Chemicon, Millipore
Histone 3 (phospho S10)	Mytosis marker	1:200	Rabbit polyclonal	Abcam

© 2011 The Authors; Brain Pathology © 2011 International Society of Neuropathology

antibodies (Table 1) diluted in incubation buffer. Sections were then incubated in incubation buffer containing the corresponding fluorescent (1:1000, Invitrogen, Paisley, UK; 1:250, Jackson Labs, Bar Harbor, ME, USA) or biotinylated (1:200, Vector) secondary antibodies for 1 h at RT, and subsequently with the Vectastain Elite ABC reagent (Vector) where necessary. The peroxidise reaction product was visualized with 0.05% 3,3′-diaminobenzidine (Sigma) and 0.003% H_2O_2 in 0.1 M Tris-HCl (pH 7.6). The reaction was monitored under a microscope and terminated by rinsing the slides with PB. For immunofluorescence, cell nuclei were stained with Hoechst 33342 (10 μg/mL, Sigma). Control tissue was incubated without the primary antibody and no staining was observed.

Apoptosis assay

Assessment of apoptosis was performed by TUNEL analysis using the ApoTag® Plus Fluorescein *in situ* Apoptosis Detection Kit (Millipore, Billerica, MA, USA), according to manufacturer's instructions.

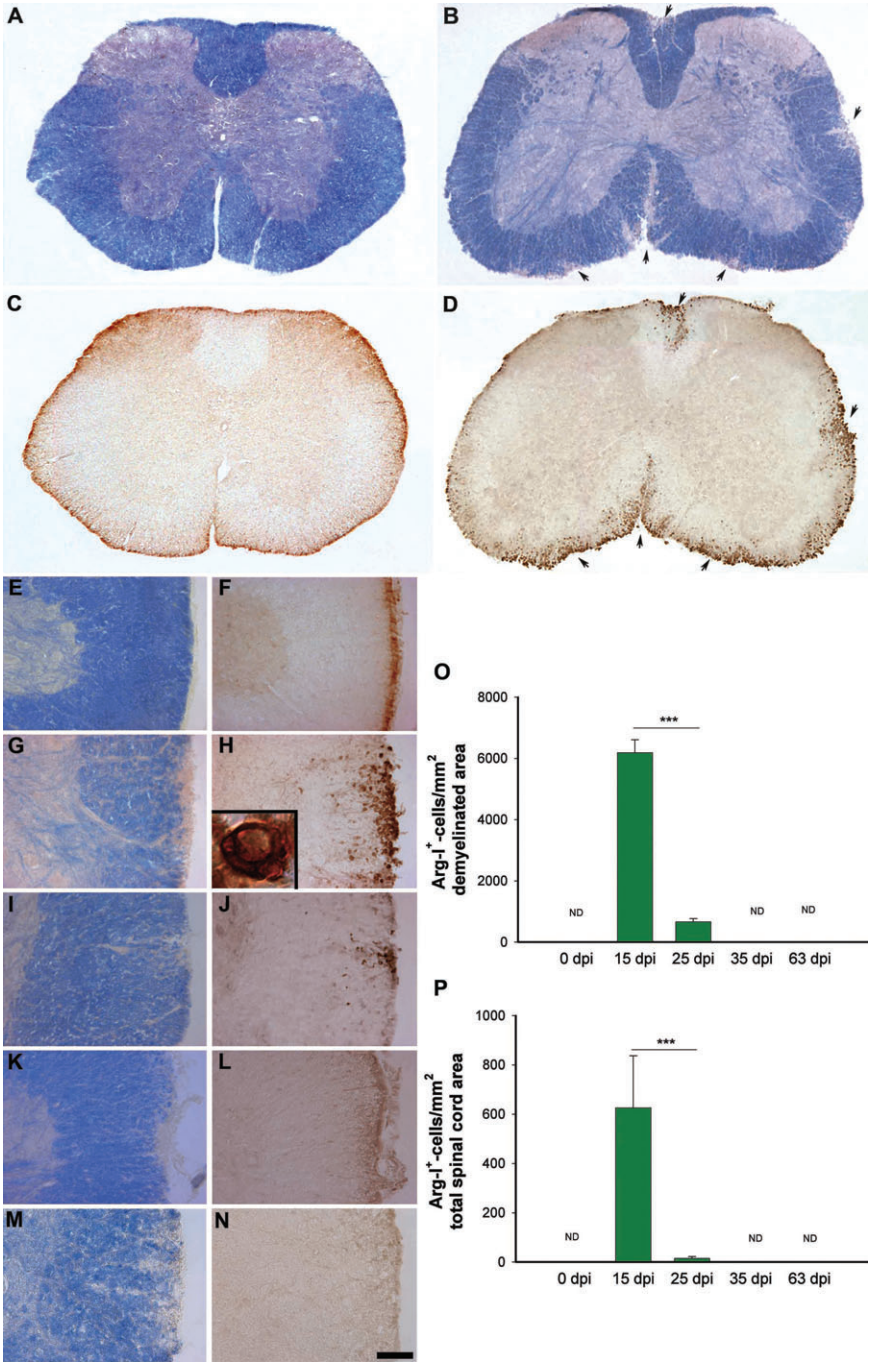

Figure 1. *Arg-I expression parallels the time course of EAE*. **A–D**. Panoramic views of sham (**A**, **C**) and MOG-immunized (**B**, **D**) EAE mice (clinical score: 3). Arg-I+-cells were restricted to demyelinated areas in EAE animals (arrows in **B**, **D**) and they were never observed in sham animals. **E–F**. Detailed views of parallel sections from the spinal cord, showing myelin (eriochrome cyanine staining; **E**, **G**, **I**, **K**, **M**) and Arg-I (**F**, **H**, **J**, **L**, **N**) expression in sham (**E–F**) and MOG-immunized mice at 15 dpi (**G–H**, clinical score: 3), 25 dpi (**I–J**, clinical score: 2), 35 dpi (**K–L**, clinical score: 1.5) and 63 dpi (**M–N**, clinical score: 1.5). Arg-I+-cells were closely associated with the demyelinated area at 15 dpi and 25 dpi and in cells with a round vacuolated cytoplasm (inset in **H**). **O–P**. Quantification of the Arg-I+-cells in the demyelinated area (**O**) or the whole spinal cord surface (**P**). Arg-I+-cell density peaked at 15 dpi, it fell significantly at 25 dpi and disappeared from 35 dpi onwards. For all experimental groups the results were analyzed by the Student's *t*-test with a critical value of ***$P < 0.001$ (25 *vs.* 15 dpi). ND: Not determined. Scale bar: A–D = 110 μm; E–N = 50 μm; inset in H = 17 μm.

© 2011 The Authors; Brain Pathology © 2011 International Society of Neuropathology

Isolation of splenic T lymphocytes

Splenocytes from control C57BL/6 mice were obtained as described previously (55). For T lymphocyte isolation, 40×10^6 splenocytes were resuspended in sterile 1X PBS with 2% bovine serum albumin (BSA), 5% fetal bovine serum (FBS) and 2% Penicillin/Streptomycin (sorting buffer), and the Fc receptors were blocked with anti-CD16/CD32 antibodies (BD Biosciences, Franklin Lakes, NJ, USA) for 10 min at 4°C. After blocking, fluorescein isothiocyanate (FITC)-conjugated anti-CD3ε (BD Biosciences) antibody were added to the cell suspension and incubated for 30 min at 4°C in the dark. Splenocytes were then washed twice

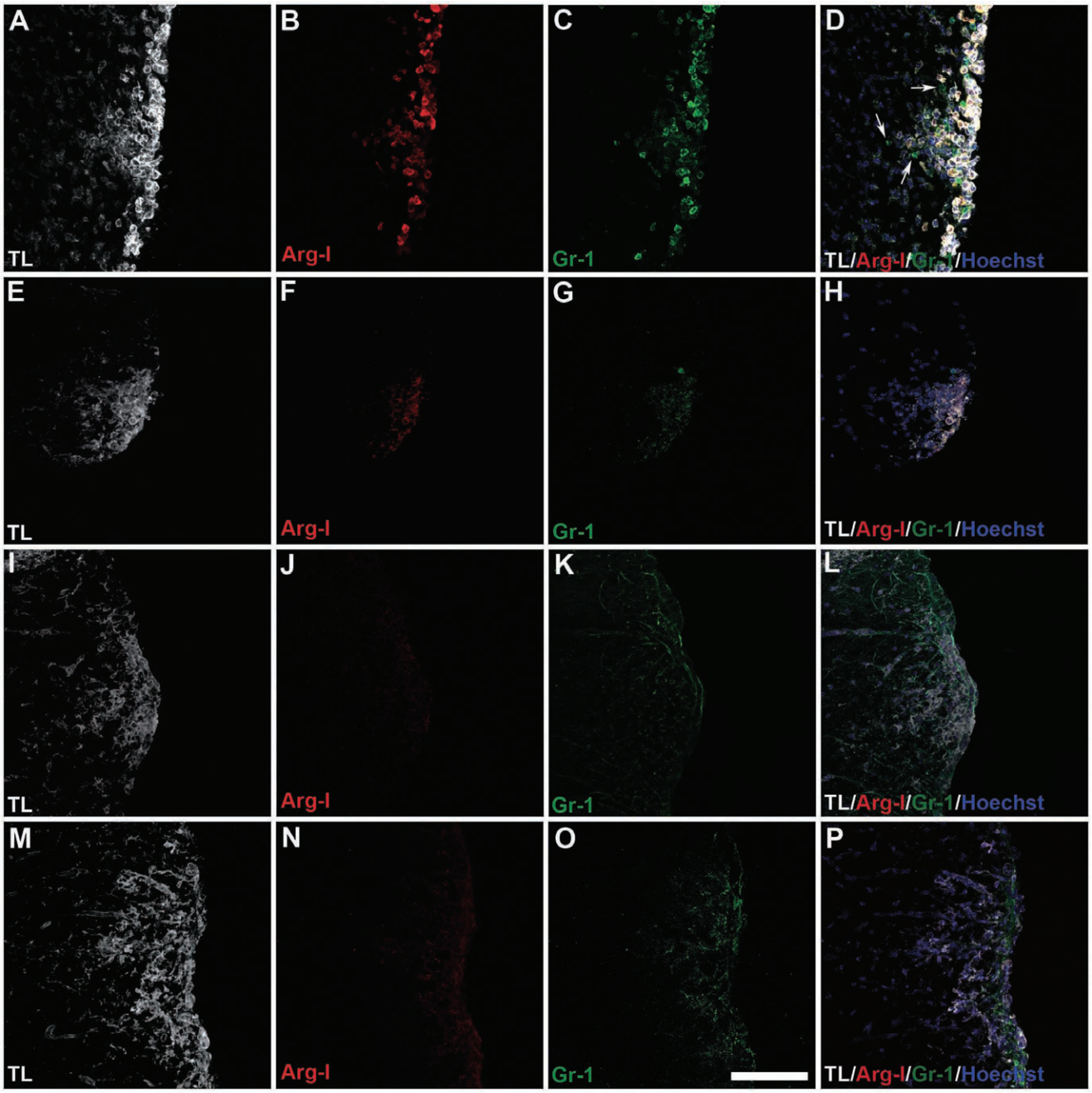

Figure 2. *Arg-I$^+$-cells expressed Gr-1 during EAE.* **A–P**. Expression of Arg-I (**B**, **F**, **J**, **N**) and Gr-1 (**C**, **G**, **K**, **O**) during EAE at 15 dpi (**A**–**D**, clinical score: 3), 25 dpi (**E**–**H**, clinical score: 1.5), 35 dpi (**I**–**L**, clinical score: 2) and 63 dpi (**M**–**P**, clinical score: 1.5). Cell infiltrates were labelled with tomato lectin (TL). Demyelinated lesions appeared full of TL$^+$-cells (**A**, **E**, **I**, **M**) at all the time points analyzed. Co-localization studies (**D**, **H**, **L**, **P**) revealed that Arg-I$^+$-cells represented a subpopulation of both the inflammatory infiltrate and the Gr-1$^+$-cell populations. Arg-I$^-$/Gr-1$^+$ cells were strongly stained (arrows in D). Scale bar: A–P = 50 μm.

© 2011 The Authors; Brain Pathology © 2011 International Society of Neuropathology

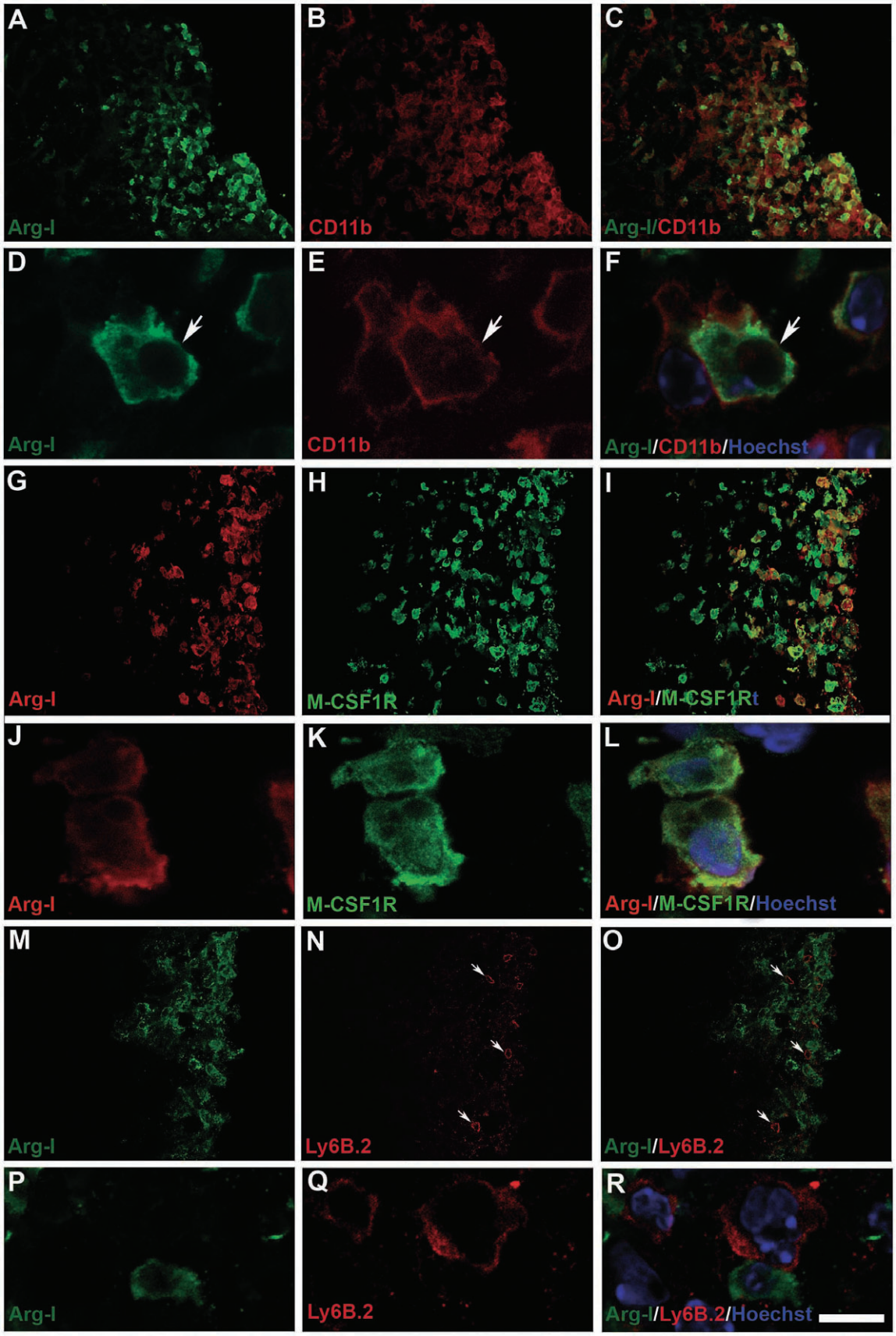

© 2011 The Authors; Brain Pathology © 2011 International Society of Neuropathology

with sorting buffer, centrifuged at 1500 rpm for 5 min at RT and sorted in a fluorescence activated cell sorting (FACS) Aria cell sorter (BD Bioscience). $CD3^+$-cells were selected and recovered at a purity > 95%.

CNS MDSC cell isolation

For each experiment, four MOG-immunized animals with a maximal EAE clinical score (3–3.5) and the corresponding sham animals, were sacrificed and perfused with PBS. The spinal cord was dissected out of each mouse, cut into small pieces and digested for 45 min at 37°C with gentle shaking in Ca^{2+}- and Mg^{2+}-free Hanks' balanced salt solution (HBSS) solution containing 400 U/mL collagenase VII (Sigma), 1% DNase (Sigma) and 100 mM $CaCl_2$. The tissue was mechanically homogenized and centrifuged at 2000 rpm for 5 min at RT. To remove myelin and obtain the cellular infiltrates, the pellet was resuspended in 70% percoll (Sigma) and loaded onto a gradient tube with 1 mL 70% percoll, 1.5 mL 30% percoll and 0.5 mL sterile 1X PBS. After centrifugation at 2600 rpm for 30 min, myelin was removed and CNS inflammatory cells were retrieved from the 30/70% interface. The cell suspension was passed through a 70 μm nylon strainer (BD Biosciences) and washed twice in sorting buffer (without BSA). After blocking Fc receptors (as described above), CNS inflammatory cells were incubated with the following antibodies: Pacific Blue-conjugated hamster anti-mouse CD3ε, FITC-conjugated rat anti-mouse Ly-6C, R-PE-conjugated rat anti-mouse Ly-6G and PerCP-Cy5.5-conjugated rat anti-mouse CD11b (all from BD Biosciences). Cell samples were analyzed in a FACS Aria cell sorter using FACS Diva 6.1 software. The $Ly\text{-}6C^{hi}/Ly\text{-}6G^{-/low}$ subpopulation was isolated from the $CD3^-/CD11b^+$-gated population, and the purity was >95%.

T cell and MDSC co-culture and cell cycle analysis

Flat bottom 96-well plates were coated with anti-CD3/CD28 antibodies (1 μg/mL each) for 3 h at 37°C. Purified $CD3^+$-T cells were plated at a density of 2×10^5 cells/well and stimulated for 24 h with anti-CD3/CD28. Pre-activated T cells were then cultured alone or with 1×10^5 MDSCs/well in the presence of plate-bound anti-CD3/CD28. After 48 h, the cells were recovered by centrifugation at 2000 rpm at RT, washed in 1X PBS and fixed in 70% EtOH at –20°C. The cells were stained with a propidium iodide/RNase solution (Immunostep, Salamanca, Spain) according to the manufacturer's instructions and the cell cycle was analyzed in a FACS Canto II cytometer with FACS Diva 6.1 software, recording 30 000 events.

Cell count, distance measurement and statistical analysis

The total number of cells of interest was assessed using a confocal microscope manually counting cells in 12 sections from all the demyelinated areas of the spinal cord (visualized by MBP immunohistochemistry), each separated by 340 μm. Twelve pictures were taken at different levels of each demyelinated area to avoid cell count repetitions. The total number of cells was considered in relation to the demyelinated area or to the whole spinal cord area (both measured using ImageJ software). The Leica Application Suite 2.7.0 R1 was used to measure distances. The data were expressed as the mean ± SEM, and they were analyzed with SigmaStat (SPSS Inc., Chicago, IL, USA). The Student's *t*-test was used to compare the groups in which stained cells appeared (15 dpi and 25 dpi, see below in Results). For correlation analysis, Pearson Product Moment was performed. Minimal statistical significance was set at $P < 0.05$ and the results were represented as follows: *, <0.05; **, <0.01; ***, <0.001.

RESULTS

Arg-I-expressing cells are present in the spinal cord of MOG-immunized mice

Whereas no Arg-I^+-cells were detected in control or sham animals at any stage (Figure 1A,C,E–F), a population of these cells was identified in the spinal cord of immunized animals at 15 dpi and 25 dpi (Figure 1B,D,G–J). Arg-I^+-cells had different shapes (from round to polygonal; diameter of 7.78 ± 0.15 μm) and staining intensities, and they had a vacuolated cytoplasm (Figure 1H). These cells were always detected in close association with demyelinating lesions and more frequently within the demyelinated area than in the surrounding area, so-called the periplaque (Figure 1G–J). From 35 dpi onwards, Arg-I^+-cells had disappeared entirely from this tissue (Figure 1 K–N). Comparing both stages in which Arg-I^+-cells were present, the number of positive cells *per* area of demyelination or *per* total area of spinal cord was significantly higher at 15 dpi than at 25 dpi (Figure 1O–P), which paralleled with the clinical course of EAE.

Arg-I-positive cells exhibit characteristics of MDSCs

Several markers have been characterized in MDSCs from different disease models (15, 18, 27, 32, 34, 38), including mouse demyelinating models (6, 44, 55), and in all cases, MDSCs always expressed both Gr-1 and CD11b. In the spinal cord of EAE mice, no Gr-1

Figure 3. *Arg-I^+-cells within the spinal cord presented the characteristic MDSC phenotype.* **A–C**. Panoramic view of one demyelinated lesion at 15 dpi (clinical score: 3). Arg-I^+-cells (**A**) comprised a subpopulation of $CD11b^+$-cells (**B**, merged in **C**). **D–F**. High magnification of Arg-I^+- (**D**) and $CD11b^+$- (**E**) double-labelled cells from a cell infiltrate at 15 dpi showing the co-expression of both markers (**F**). Arrow denotes cell with clear macrophage morphology. **G–I**. Detailed view of one demyelinated lesion at 15 dpi (clinical score: 3) illustrating how Arg-I^+-cells (**G**) represent a subpopulation of M-$CSF1R^+$-cells (**H**–**I**). **J–L**. High magnification of two macrophages showing Arg-I (green) and M-CSF1R (red) expression. **M–O**. Detailed view of one demyelinating lesion at 15 dpi (clinical score: 3) demonstrating the presence of Arg-I^+-cells (**M**) and neutrophils (arrows in N–O) in completely independent subpopulations. **P–R**. Higher magnification of an EAE cell infiltrate showing the different morphologies of Arg-I^+-cells and neutrophils (with typical polymorphic nuclei). Scale bar: A–C = 60 μm; D–F = 8 μm; G–I = 55 μm; J–L = 9 μm. M–O = 50 μm; P–R = 9 μm.

© 2011 The Authors; Brain Pathology © 2011 International Society of Neuropathology

expression was observed in either control or sham mice at any of the stages studied (Supporting Information Figure S1A–C). However, as EAE progressed, Gr-1$^+$-cells were observed within and around the demyelinated area of the spinal cord at the same stages at which Arg-I was detected (Figure 2A–H). Moreover, these cells disappeared in parallel with the Arg-I immunostaining (Figure 2I–P). Indeed, Arg-I$^+$-cells comprised a subpopulation of Gr-1$^+$-cells that were both strongly and weakly stained, although most Gr-1$^+$/Arg-I-cells exhibited strong staining (Figure 2A–D). Although the density of Gr-1$^+$-cells was higher at 15 dpi than at 25 dpi (Supporting Information Figure S2A), the percentage of Gr-1$^+$-cells exhibiting Arg-I-immunoreactivity with respect to the total Gr-1$^+$-cells did not vary between these periods (Supporting Information Figure S2B).

CD11b was present in microglial cells from both control and sham animals (Supporting Information Figure S1D–F). Moreover, at all stages of EAE studied, CD11b was detected at different intensities in infiltrated round or polygonal cells, as well as in activated microglia. At both 15 dpi and 25 dpi, Arg-I$^+$-cells represented a subpopulation of the CD11b$^+$-cells (Figure 3A–F). As with Gr-1, no correlation was observed between Arg-I immunore-

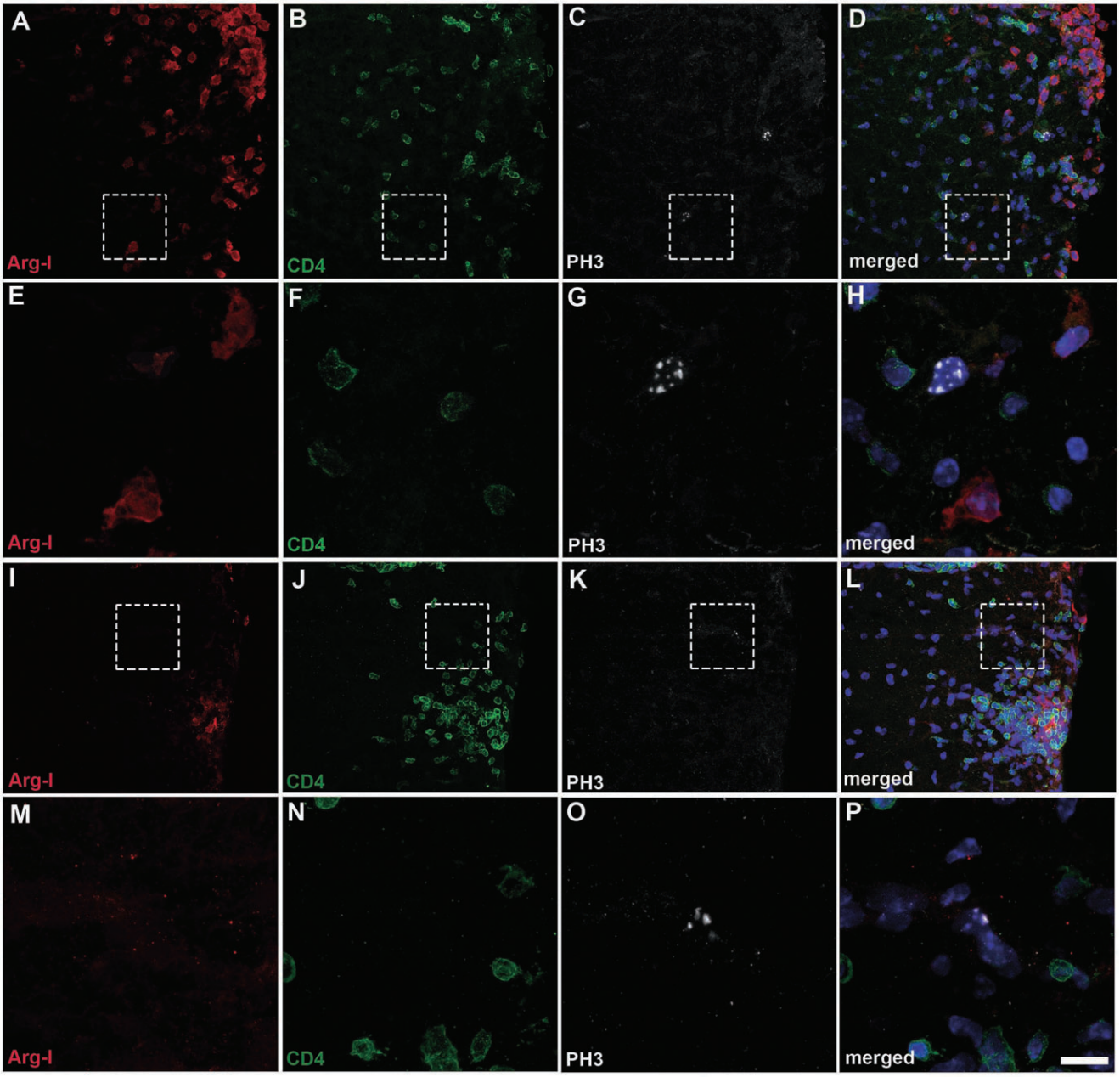

Figure 4. *The presence of Arg-I$^+$-cells is independent of the proliferative state of lymphocytes during EAE.* In the spinal cord, neither Arg-I$^+$-MDSCs (**A**, **E**, **I**, **M**) nor lymphocytes (**B**, **F**, **J**, **N**) present the mitotic marker phosphohistone H3 (PH3: **C–D**, **G–H**, **K–L**, **O–P**) at the peak clinical score (15 dpi, **A–H**) or after the limitation of the immune response (25 dpi, **I–P**). Scale bar: A–D, I–L = 40 μm; E–H, M–P = 10 μm.

© 2011 The Authors; Brain Pathology © 2011 International Society of Neuropathology

activity and the intensity of CD11b staining, and the density of CD11b$^+$-cells paralleled the clinical score attributed to the animals (Supporting Information Figure S2C). In contrast, no variations were observed in the percentage of CD11b$^+$/Arg-I$^+$-cells with respect to total CD11b$^+$-cells (Supporting Information Figure S2D).

Together with CD11b and Gr-1, the macrophage-colony stimulating factor 1 receptor (M-CSF1R), also known as CD115, has been considered as an additional marker for a subset of highly suppressive MDSCs (28), as well as a characteristic marker of immature cells of the monocyte/macrophage lineage (43). In our model, microglial cells from both control and sham animals

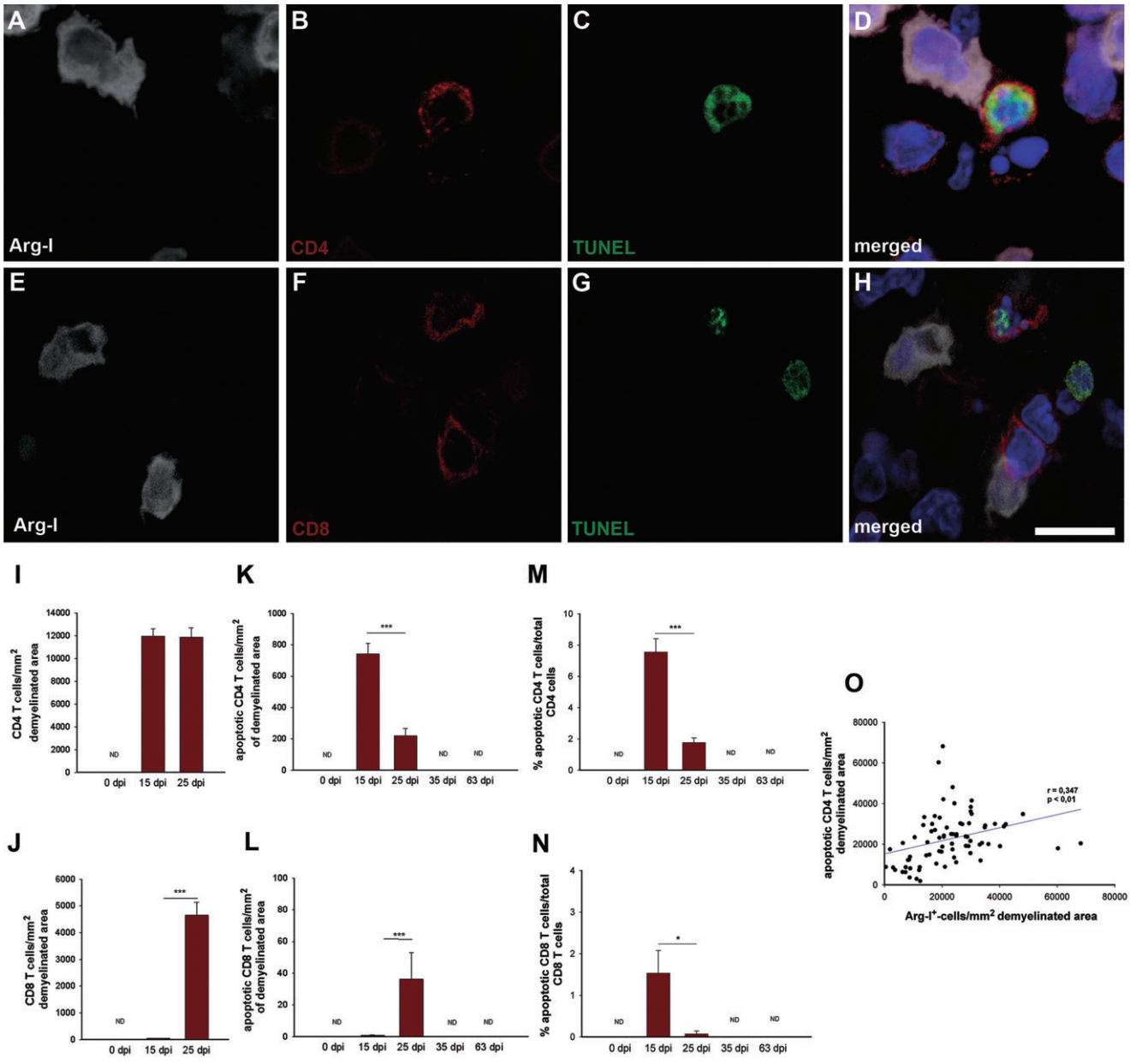

Figure 5. *Arg-I$^+$-MDSCs in EAE are involved in T lymphocyte apoptosis.* **A–H**. Example of an Arg-I$^+$-MDSC in direct contact with an apoptotic CD4 T cell (**A–D**), or in proximity to a CD8 T cell (**E–H**), within a demyelinated spinal cord lesion at 15 dpi (clinical score: 3). **I–J**. Quantification of the total number of CD4 (**I**) and CD8 (**J**) T cells at those time points at which Arg-I$^+$-MDSCs were observed (15 dpi and 25 dpi). Although the demyelinated areas showed equal CD4 T cell densities at both stages analyzed, the density of CD8 T cells was significantly higher at 25 dpi versus 15 dpi. **K–L**. The density of apoptotic CD4 T cells was significantly higher at 15 versus 25 dpi (**K**), in contrast to that observed for apoptotic CD8 T cells (**L**). **M–N**. The proportion of apoptotic CD4 (**M**) or CD8 (**N**) T cells was significantly higher at 15 dpi versus 25 dpi. For all experimental groups the results were analyzed by Student's *t*-test with critical values of $*P < 0.05$ and $***P < 0.001$ (25 dpi versus 15 dpi). **O**. Pearson's test of the density of Arg-I$^+$- and apoptotic CD4 T cells revealed a significant positive correlation. ND: Not determined. Scale bar: A–D = 10 μm; E–H = 9 μm.

© 2011 The Authors; Brain Pathology © 2011 International Society of Neuropathology

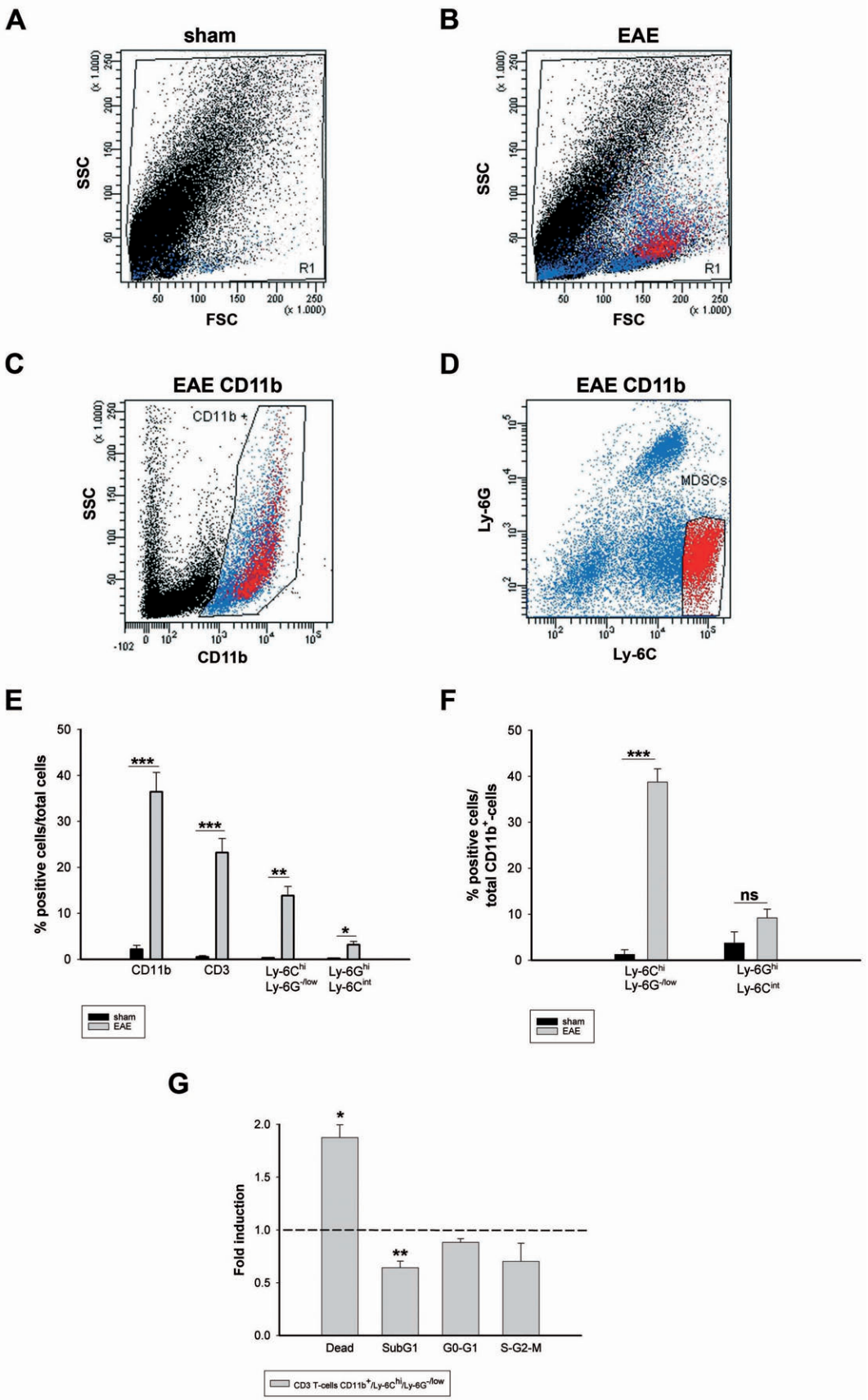

© 2011 The Authors; Brain Pathology © 2011 International Society of Neuropathology

Table 2. Percentage and location of apoptotic T cells around an Arg-I$^+$-cell.

dpi	% Apoptotic CD4 T cells			% Apoptotic CD8 T cells		
	In contact	Near	Far	In contact	Near	Far
15	73,4	25,4	1,2	68,75	31,25	0
25	26,4	29,4	44,2	100	0	0

Near = <5 μm from an Arg-I$^+$-cell; Far = ≥5 μm from an Arg-I$^+$-cell; dpi = days post-immunization.

exhibited weak M-CSF1R labelling, mainly in their processes, at all stages analyzed (Supporting Information Figure S1G–I). Strong immunolabelling of well-vacuolated round or polygonal cells, which were readily identified as infiltrated monocytes that were not present in control or sham animals, was detected within the demyelinated area and in the periplaque (Figure 3G–L). As described for Gr-1$^+$- and CD11b$^+$-cells, the density of M-CSF1R$^+$-cells was significantly higher at 15 dpi than at 25 dpi (Supporting Information Figure S2E). In contrast, the percentage of double-labelled M-CSF1R$^+$/Arg-I$^+$-cells, with respect to total M-CSF1R$^+$-cells, remained constant in these two stages (Supporting Information Figure S2F). Their monocytic characteristics were also corroborated by the absence of the specific neutrophil marker Ly-6B.2 (51) in Arg-I$^+$-cells (Figure 3 M–R). Thus, as for CD11b and Gr-1, a subpopulation of M-CSF1R$^+$-cells expressed Arg-I, allowing us to classify them as highly suppressive MDSCs with macrophage-monocyte morphological and cytochemical characteristics.

The presence of Arg-I$^+$-cells is associated with apoptosis of T lymphocytes

MDSCs are proposed to exert their suppressive effects on T cell populations in two ways: by reducing T cell proliferation and inducing T cell apoptosis (9, 44). At the stages in which Arg-I$^+$-cells were evident in the spinal cord (15 dpi and 25 dpi), no mitotic lymphocytes were observed (cells labelled with phosphohistone H3, PH3: Figure 4A–D,I–L). Moreover, the few PH3$^+$-cells detected displayed neither Arg-I nor the CD4/CD8 T lymphocyte markers (Figure 4E–H,M–P and data not shown).

Apoptotic CD4 and CD8 T cells were detected exclusively at 15 dpi and 25 dpi, when Arg-I$^+$-MDSCs were observed. At both stages, apoptotic T cells were detected in contact with or near to an Arg-I$^+$-MDSC (no further than 5 μm: Figure 5A–H). Interestingly, cell–cell contact-mediated apoptosis is thought to be a mechanism by which MDSCs exert their suppressive function (2). During EAE, the distribution of apoptotic CD4 and CD8 T cells was altered with respect to Arg-I$^+$-cells (see Table 2 for details). Whereas at 15 dpi most apoptotic CD4 T cells were in direct contact with or in the proximity of an Arg-I$^+$-MDSC, by 25 dpi the percentage of apoptotic CD4 T lymphocytes directly in contact with an Arg-I$^+$-cell decreased, although the number in close proximity to an Arg-I-expressing MDSC remained stable (Table 2). As the total number of CD4 T cells was the same at both points when the apoptotic profiles were analyzed (Figure 5I), the total number and the percentage of apoptotic CD4 T cells was significantly higher at 15 dpi than at 25 dpi (Figure 5K,M). Moreover, while a direct correlation between the total numbers of Arg-I$^+$-cells and apoptotic CD4 T cells was observed at 15 dpi (Figure 5O), this correlation was not seen at 25 dpi.

A clear change in the distribution of apoptotic CD8 T cells occurred between 15 dpi and 25 dpi (see Table 2 for details). Although at both stages all double-labelled cells were in close proximity to an Arg-I$^+$-cell, some of them did not directly contact these cells at 15 dpi, but all were in direct contact at 25 dpi. The total number of CD8 T cells (Figure 5J) and apoptotic CD8 T cells (Figure 5L) was lower at 15 dpi than at 25 dpi, whereas like apoptotic CD4 T cells, the percentage of apoptotic CD8 T cells was significantly higher at 15 dpi than at 25 dpi (Figure 5N). Moreover, there was no correlation between the number of Arg-I$^+$-MDSCs and the density or percentage of apoptotic CD8 T cells (not shown).

MDSCs from the spinal cord of EAE mice induce T lymphocyte death

To corroborate our previous morphological observations, the presence and composition of inflammatory infiltrates in the spinal cords of sham and immunized mice (those with a peak clinical score, 3–3.5) were analyzed by flow cytometry. There was a population of infiltrated cells in MOG-immunized mice that was not detected in sham animals (Figure 6A–B). To characterize the cellular infiltrates by flow cytometry, T lymphocytes and myeloid cells were identified by CD3 and CD11b expression, respectively (Figure 6C–D, blue population). There was a significant increase in the total proportion of myeloid cells (CD11b$^+$-cells; blue population, Figure 6A–D) and T lymphocytes (CD3$^+$-cells) in EAE mice when compared with sham animals (Figure 6E). In EAE, MDSCs and neutrophils were previously characterized by flow cytometry on the basis of Ly-6C and Ly-6G antigen expression (the two antigens recognized by anti-Gr-1 antibody) (44, 55). MDSCs presented a CD11b$^+$/Ly-6C^{hi}/

Figure 6. *MDSCs extracted from the spinal cord of immunized mice promote T cell death.* **A–B**. The spinal cord of MOG-immunized mice (**B**) at the peak clinical score contained a larger population of infiltrated cells (colored events) than that of sham animals (**A**). **C–D**. CD11b expression was analyzed in the CD3$^-$-population (**C**). CD11b$^+$-cells (blue) were gated, and Ly-6C and Ly-6G surface expression was analyzed. The MDSC gate contained CD11b$^+$/Ly-6C^{hi}/Ly-6G$^{-/low}$ cells (colored in red in D). **E**. In the spinal cord, the percentage of CD11b, CD3, Ly-6C^{hi}/Ly-6G$^{-/low}$ and Ly-6G^{hi}/Ly-6C^{int} cells with respect to the total infiltrated cells was significantly higher in MOG-immunized versus sham mice at the peak clinical score (15 dpi). **F**. The percentage of Ly-6C^{hi}/Ly-6G$^{-/low}$ cells (MDSCs) with respect to total myeloid cells (CD11b$^+$) was significantly higher in the spinal cord of MOG-immunized versus sham mice, whereas no significant differences in Ly-6G^{hi}/Ly-6C^{int} cells (neutrophils) were detected between groups. **G**. The presence of MDSCs extracted from the spinal cord of MOG-immunized mice at the peak clinical score induced a significant increase in the proportion of dead T cells and a significant decrease in the percentage of SubG1 T cells. In contrast, no significant variations were observed in the proportion of viable cells (G0-G1 or S-G2-M). The results were analyzed with the Student's *t* test applying the critical values of $P < 0.05$ (*), $P < 0.01$ (**) and $P < 0.001$ (***). ns = not significant.

© 2011 The Authors; Brain Pathology © 2011 International Society of Neuropathology

Ly-6G$^{-/low}$ phenotype, whereas neutrophils presented a CD11b^{+}/Ly-6G^{hi}/Ly-6C^{int} phenotype. We identified both subpopulations in the spinal cord of MOG-immunized mice (Figure 6C–D), and the proportion of both MDSCs and neutrophils was significantly higher in immunized mice than in sham animals (Figure 6E). In contrast, only MDSCs augmented significantly with respect to the total number of CD11b^{+}-cells in EAE animals (Figure 6F).

Important immunosuppressive effects have been attributed to the myeloid CD11b^{+}/Ly-6C^{hi}/Ly-6G$^{-/low}$ subpopulation extracted from the spleen of Balb/C EAE mice (55). To determine whether this subpopulation exhibited similar characteristics when isolated from the spinal cord of EAE mice with a peak clinical score, anti-CD3/CD28 stimulated splenic CD3^{+}-cells from control mice were exposed to MDSCs. After 48 h in co-culture, the cell cycle stage of the CD3 cells was analyzed using a propidium iodide/RNase assay, revealing a significant increase in the percentage of dead cells (Figure 6G). A significant decrease in the proportion of CD3^{+}-stimulated cells in the SubG$_1$ phase was also detected in the presence of MDSCs (Figure 6G). In contrast, there was no significant variation in the cells in either the G$_0$-G$_1$ or the S-G$_2$-M phases (Figure 6G). Together, the changes observed in lymphocytes when co-cultured with the CD11b^{+}/Ly-6C^{hi}/Ly-6G$^{-/low}$ cells isolated from the spinal cord of EAE animals confirm that these cells exhibit the functional, as well as morphological and phenotypic characteristics of MDSCs.

DISCUSSION

This is the first characterization of the presence and distribution of Arg-I^{+}-cells within the spinal cord of EAE mice. In this study, Arg-I^{+}-cell number peaked during the active phase (15 dpi) and it decreased when the immune response became limited (25 dpi), disappearing during the chronic period (35 dpi onwards). This pattern is in accordance with the expression of *Arg-I* mRNA described elsewhere (52). The number of Arg-I^{+}-cells appeared to parallel the clinical score of EAE mice and the different phases of EAE. Indeed, Arg-I^{+}-cells were detected exclusively when the switch from pro-inflammatory to anti-inflammatory conditions occurs and the active phase ends, limiting the immune response (1, 4, 22, 27, 45). Arg-I^{+}-cells also expressed CD11b and Gr-1 (typical markers of monocyte-derived cells and granulocytes, respectively), allowing us to morphologically classify them as MDSCs (cells with intermediate characteristics between monocyte-derived cells and granulocytes). These two markers (CD11b and Gr-1) have been used previously to classify and detect MDSCs in different pathological conditions (6, 14, 23, 27, 34, 44, 48), including those isolated from the spleen of Balb/C EAE mice (55). It is now known that commonly employed anti-Gr-1 antibodies recognize two complementary antigens, Ly-6C and Ly-6G (38, 53). Indeed, during EAE in Balb/C mice, MDSCs have been identified as Ly-6C^{hi}/Ly-6G^{-} cells (55). Although we observed an increase in Ly-6C^{hi}/Ly-6G$^{-/low}$ cells in the spinal cord of C57/BL6 EAE mice, we were unable to identify differences in their immunohistochemical intensity in the CNS, as our Gr-1 antibody does not distinguish between both markers. Nonetheless, we chose M-CSF1R (also known as CD115) as an additional MDSC marker caused by its specificity as a monocyte lineage marker (21, 43). Our data demonstrating that Arg-I and M-CSF1R were co-expressed, corroborate previous observations regarding the monocytic nature of MDSCs isolated from the spleen in EAE (55). Moreover, the Gr-1/M-CSF1R combination has been demonstrated as a better option to identify MDSCs with the highest suppressive activity among all CD11b^{+}/Gr-1^{+}-cells (28). One of the MDSC stimulating factors is macrophage-colony stimulating factor (M-CSF) (10), whose receptor M-CSF1R (also known as CD115) was identified in our Arg-I^{+}-MDSCs. In addition, we ruled out a possible neutrophilic nature of Arg-I^{+}-suppressive cells (54) based on their morphological characteristics and the lack of expression of the polymorphonuclear cell marker Ly-6B.2. Indeed, Arg-I^{+}- and Ly-6B.2^{+}-cells were two completely independent cell populations. The scarce Gr-1^{+}-cells that did not display Arg-I immunoreactivity showed a high staining intensity of the granulocyte marker, which could indicate their more end-stage neutrophile profile (26). In our experimental conditions, we found that M-CSF1R, CD11b and Gr-1 were expressed by all Arg-I^{+}-MDSCs at both 15 dpi and 25 dpi, indicating that Arg-I may be a useful marker for the most immunosuppressive monocyte-derived MDSCs in CNS tissue. Indeed, these Arg-I^{+}-MDSCs may be responsible for the dramatic increase in *Arg-I* expression observed in EAE (52).We found a direct correlation *in situ* between the spatio-temporal distribution of Arg-I^{+}-MDSCs and that of apoptotic T lymphocytes in the spinal cord during EAE. Both cell types were only evident at 15 dpi and 25 dpi, although more Arg-I^{+}-MDSCs were detected at 15 dpi (Figure 7), and both cell types were largely restricted to the demy-

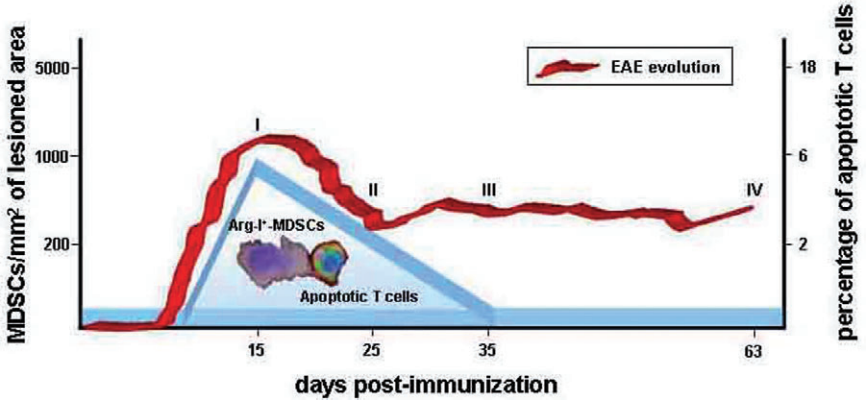

Figure 7. *The presence of Arg-I^{+}-MDSCs parallels the time course of EAE.* The density of Arg-I^{+}-MDSCs parallels the changes in both the percentage of apoptotic T cells and the clinical score of EAE animals. (I) The highest density of MDSCs and proportion of apoptotic T cells occurred at the peak clinical score (15 dpi). (II) Both these parameters decreased after the immune response was limited (25 dpi). At the beginning of the chronic phase (III; 35 dpi) or the end of the analyzed time course (IV; 63 dpi) the animals remained symptomatic, although neither Arg-I^{+}-MDSCs nor apoptotic lymphocytes were detected.

© 2011 The Authors; Brain Pathology © 2011 International Society of Neuropathology

elinated area. Notably, MDSCs are extremely potent inhibitors of T cell proliferation *in vitro*, acting by down-regulating the CD3ζ-chain (40). Thus, the immediate function of MDSCs in EAE appears to be to prevent activated T cells from entering the cell cycle without inducing their own cell apoptosis. Although blocking proliferation would eventually lead to apoptotic cell death (2, 55), the absence of the mitotic marker PH3 in T lymphocytes in the spinal cord of immunized animals, together with the insignificant variation in the number of T cells that remained in cell cycle, points to distinct suppressor activity of MDSCs once they enter the CNS. Our data show that at 15 dpi and 25 dpi, most (if not all) apoptotic CD4 or CD8 T cells were in direct contact with an Arg-I$^+$-MDSC. Although reports are controversial about whether MDSCs exclusively provoke T lymphocyte apoptosis through cell–cell contact (2, 49, 53), our data in EAE point to this imperative requirement as we demonstrate this important morphological feature for the first time in the CNS (53). This was corroborated in our co-cultures of MDSCs and T cells as the presence of MDSCs isolated from EAE spinal cord at the peak clinical score enhanced the death of activated lymphocytes.

The parallel between the number and distribution of Arg-I$^+$-MDSCs at the peak stage of EAE (15 dpi) and their self-limitation after inflammation (25 dpi; Figure 7) are striking morphological and functional correlations. In our EAE model, a slight clinical improvement was observed after 15 dpi. This recuperation has been attributed to a change in the inflammatory environment, which shifts its composition toward Th2 cytokines (1, 3, 5, 50). It is clear that the suppressor activity of MDSCs requires factors derived from activated T cells that promote their activation, including IL-4 and IL-13, which mediate Arg-I up-regulation in MDSCs (8, 27, 41). The increased activity of Arg-I in MDSCs enhances L-arginine catabolism, depleting this semi-essential amino acid from the microenvironment (9). Such a situation would be promoted when the number of Arg-I$^+$-MDSCs is increased, as seen in the present study. The shortage of L-arginine induces a decrease in CD3ζ expression in T cells and, subsequently, the inhibition of T cell proliferation and induction of T cell apoptosis (9, 18). Our study is the first to explore the immunosuppressive nature of MDSCs directly extracted from the spinal cord rather than from the spleen: within the CNS, MDSCs mainly affect the survival rather than the proliferation of T cells.

Our data are consistent with previous reports describing the importance of MDSCs in EAE. Intravenously applied myeloid precursors transduced with microglial TREM2 (triggering receptor expressed on myeloid cells-2) ameliorate clinical symptoms and induce recovery from EAE (47). These cells were seen to migrate into the CNS lesions, induce the clearance of myelin debris and create an anti-inflammatory cytokine milieu. In addition, the absence of CNS-derived IL-4, one of the most potent inducers of Arg-I expression (36), results in a more severe EAE and an increase in the number of infiltrating cells (39).

Myeloid precursors with the typical MDSC phenotype (CD11b/CD115/Ly-6C^{hi}) are also precursors of dendritic cells and M1 macrophages (cells with pro-inflammatory activity) in EAE lesions, but without showing Arg-I immunoreactivity (30). An explanation for this apparent contradiction may be found in the different microenvironments established in the CNS during the active versus remitting/chronic phases of EAE. During the active phase of EAE, the molecular environment gives rise to pro-inflammatory dendritic/macrophagic cells that promote Th1 and Th17 polarization. It is possible that the CNS microenvironment evolves during the course of the disease, such that infiltrating immature monocytes are induced to adopt an innocuous or even immunosuppressive phenotype when clinical remission takes place, as evident through the induction of Arg-I by CD11b/Gr-1/M-CSF1R cells. Our data suggest that both subsets of monocyte-derived cells (dendritic/macrophagic cells and MDSCs) could co-exist during EAE, as Arg-I$^+$-cells represent only a subpopulation of the CD11b$^+$-, Gr-1$^+$- and M-CSF1R$^+$-cells.

Together, our data demonstrate that Arg-I is a useful marker to discriminate a particular subpopulation of immature monocytes (MDSCs) that modulates the immune response and that promotes T cell apoptosis at a stage when inflammatory damage is limited. The findings obtained from the EAE model point to the pharmacogenetic manipulation and transplantation of this specific Arg-I$^+$-MDSC population as a promising therapeutic strategy to effectively treat MS patients, thereby reducing the side effects that general Arg-I inactivation may produce.

ACKNOWLEDGMENTS

We thank Laura García, Amelia González, Isabel Machín and Rafael Lebrón for their technical support; Dr José Ángel Rodríguez-Alfaro for his help with the confocal imaging; Dr Iván Bernardo for his help with flow cytometry analysis and Dr Augusto Silva for providing us with the MOG peptide. This work was supported by the Ministerio de Ciencia e Innovación-MICINN (SAF2009-07842); Fondo de Investigaciones Sanitarias-FIS (partially funded by F.E.D.E.R.- European Union—"Una manera de hacer Europa") (RD07-0060-2007); and Gobierno de Castilla-La Mancha (PAI08-0242-3822; ICS06024-00, G-2008-C8; PI2009-26). VMV and MCO are FISCAM fellows (MOV-2009_JI-01 and MOV-2007_JI-20, respectively). DC, VV and FdC are hired by SESCAM.

REFERENCES

1. Angulo I, de las Heras FG, Garcia-Bustos JF (2000) Nitric oxide-producing CD11b(+)Ly-6G(Gr-1)(+)CD31(ER-MP12)(+) cells in the spleen of cyclophosphamide-treated mice: implications for T-cell responses in immunosuppressed mice. *Blood* **95**:212–220.
2. Apolloni E, Bronte V, Mazzoni A, Serafini P, Cabrelle A, Segal DM *et al* (2000) Immortalized myeloid suppressor cells trigger apoptosis in antigen-activated T lymphocytes. *J Immunol* **165**:6723–6730.
3. Begolka WS, Miller SD (1998) Cytokines as intrinsic and exogenous regulators of pathogenesis in experimental autoimmune encephalomyelitis. *Res Immunol* **149**:771–781.
4. Benveniste EN (1997) Role of macrophages/microglia in multiple sclerosis and experimental allergic encephalomyelitis. *J Mol Med* **75**:165–173.
5. Bettelli E, Das MP, Howard ED, Weiner HL, Sobel RA, Kuchroo VK (1998) IL-10 is critical in the regulation of autoimmune encephalomyelitis as demonstrated by studies of IL-10- and IL-4-deficient and transgenic mice. *J Immunol* **161**:3299–3306.
6. Bowen JL, Olson JK (2009) Innate immune CD11b+Gr-1+ cells, suppressor cells, affect the immune response during Theiler's virus-induced demyelinating disease. *J Immunol* **183**:6971–6980.
7. Bronte V, Apolloni E, Cabrelle A, Ronca R, Serafini P, Zamboni P *et al* (2000) Identification of a CD11b(+)/Gr-1(+)/CD31(+) myeloid

© 2011 The Authors; Brain Pathology © 2011 International Society of Neuropathology

progenitor capable of activating or suppressing CD8(+) T cells. *Blood* **96**:3838–3846.
8. Bronte V, Serafini P, De Santo C (2003) IL-4-induced arginase 1 suppresses alloreactive T cells in tumor-bearing mice. *J Immunol* **170**:270–278.
9. Bronte V, Zanovello P (2005) Regulation of immune responses by L-arginine metabolism. *Nat Rev Immunol* **5**:641–654.
10. Bunt SK, Yang L, Sinha P, Clements VK, Leips J, Ostrand-Rosenberg S (2007) Reduced inflammation in the tumor microenvironment delays the accumulation of myeloid-derived suppressor cells and limits tumor progression. *Cancer Res* **67**:10019–10026.
11. Carmody RJ, Hilliard B, Maguschak K, Chodosh LA, Chen YH (2002) Genomic scale profiling of autoimmune inflammation in the central nervous system: the nervous response to inflammation. *J Neuroimmunol* **133**:95–107.
12. Chen ML, Yan BS, Kozoriz D, Weiner HL (2009) Novel CD8(+) Treg suppress EAE by TGF-beta- and IFN-gamma-dependent mechanisms. *Eur J Immunol* **39**:3423–3435.
13. Compston A, Coles A (2008) Multiple sclerosis. *Lancet* **372**:1502–1517.
14. Delano MJ, Scumpia PO, Weinstein JS (2007) MyD88-dependent expansion of an immature GR-1(+)CD11b(+) population induces T cell suppression and Th2 polarization in sepsis. *J Exp Med* **204**:1463–1474.
15. Dolcetti L, Peranzoni E, Ugel S, Marigo I, Fernandez GA, Mesa C *et al* (2010) Hierarchy of immunosuppressive strength among myeloid-derived suppressor cell subsets is determined by GM-CSF. *Eur J Immunol* **40**:22–35.
16. Ferber IA, Brocke S, Taylor-Edwards C, Ridgway W, Dinisco C, Steinman L *et al* (1996) Mice with a disrupted IFN-gamma gene are susceptible to the induction of experimental autoimmune encephalomyelitis (EAE). *J Immunol* **156**:5–7.
17. Frei K, Eugster HP, Bopst M, Constantinescu CS, Lavi E, Fontana A (1997) Tumor necrosis factor alpha and lymphotoxin alpha are not required for induction of acute experimental autoimmune encephalomyelitis. *J Exp Med* **185**:2177–2182.
18. Gabrilovich DI, Nagaraj S (2009) Myeloid-derived suppressor cells as regulators of the immune system. *Nat Rev Immunol* **9**:162–174.
19. Gabrilovich DI, Velders MP, Sotomayor EM, Kast WM (2001) Mechanism of immune dysfunction in cancer mediated by immature Gr-1+ myeloid cells. *J Immunol* **166**:5398–5406.
20. Gallina G, Dolcetti L, Serafini P, De SC, Marigo I, Colombo MP *et al* (2006) Tumors induce a subset of inflammatory monocytes with immunosuppressive activity on CD8+ T cells. *J Clin Invest* **116**:2777–2790.
21. Getts DR, Terry RL, Getts MT (2008) Ly6c+ "inflammatory monocytes" are microglial precursors recruited in a pathogenic manner in West Nile virus encephalitis. *J Exp Med* **205**:2319–2337.
22. Gold R, Linington C, Lassmann H (2006) Understanding pathogenesis and therapy of multiple sclerosis via animal models: 70 years of merits and culprits in experimental autoimmune encephalomyelitis research. *Brain* **129**:1953–1971.
23. Goni O, Alcaide P, Fresno M (2002) Immunosuppression during acute Trypanosoma cruzi infection: involvement of Ly6G (Gr1(+)) CD11b(+)immature myeloid suppressor cells. *Int Immunol* **14**:1125–1134.
24. Goverman J (2009) Autoimmune T cell responses in the central nervous system. *Nat Rev Immunol* **9**:393–407.
25. Groux H (2001) An overview of regulatory T cells. *Microbes Infect* **3**:883–889.
26. Hestdal K, Ruscetti FW, Ihle JN, Jacobsen SE, Dubois CM, Kopp WC *et al* (1991) Characterization and regulation of RB6-8C5 antigen expression on murine bone marrow cells. *J Immunol* **147**:22–28.
27. Highfill SL, Rodriguez PC, Zhou Q, Goetz CA, Koehn BH, Veenstra R *et al* (2010) Bone marrow myeloid-derived suppressor cells (MDSCs) inhibit graft-versus-host disease (GVHD) via an arginase-1-dependent mechanism that is up-regulated by interleukin-13. *Blood* **116**:5738–5747.
28. Huang B, Pan PY, Li Q (2006) Gr-1+CD115+ immature myeloid suppressor cells mediate the development of tumor-induced T regulatory cells and T-cell anergy in tumor-bearing host. *Cancer Res* **66**:1123–1131.
29. Jenkinson CP, Grody WW, Cederbaum SD (1996) Comparative properties of arginases. *Comp Biochem Physiol B Biochem Mol Biol* **114**:107–132.
30. King IL, Dickendesher TL, Segal BM (2009) Circulating Ly-6C+ myeloid precursors migrate to the CNS and play a pathogenic role during autoimmune demyelinating disease. *Blood* **113**:3190–3197.
31. Korn T, Bettelli E, Oukka M, Kuchroo VK (2009) IL-17 and Th17 Cells. *Annu Rev Immunol* **27**:485–517.
32. Kusmartsev SA, Li Y, Chen SH (2000) Gr-1+ myeloid cells derived from tumor-bearing mice inhibit primary T cell activation induced through CD3/CD28 costimulation. *J Immunol* **165**:779–785.
33. Liblau R, Steinman L, Brocke S (1997) Experimental autoimmune encephalomyelitis in IL-4-deficient mice. *Int Immunol* **9**:799–803.
34. Makarenkova VP, Bansal V, Matta BM (2006) CD11b+/Gr-1+ myeloid suppressor cells cause T cell dysfunction after traumatic stress. *J Immunol* **176**:2085–2094.
35. McGeachy MJ, Chen Y, Tato CM, Laurence A, Joyce-Shaikh B, Blumenschein WM *et al* (2009) The interleukin 23 receptor is essential for the terminal differentiation of interleukin 17-producing effector T helper cells *in vivo*. *Nat Immunol* **10**:314–324.
36. Munder M, Schneider H, Luckner C (2006) Suppression of T-cell functions by human granulocyte arginase. *Blood* **108**:1627–1634.
37. Murphy AC, Lalor SJ, Lynch MA, Mills KH (2010) Infiltration of Th1 and Th17 cells and activation of microglia in the CNS during the course of experimental autoimmune encephalomyelitis. *Brain Behav Immun* **24**:641–651.
38. Peranzoni E, Zilio S, Marigo I, Dolcetti L, Zanovello P, Mandruzzato S, Bronte V (2010) Myeloid-derived suppressor cell heterogeneity and subset definition. *Curr Opin Immunol* **22**:238–244.
39. Ponomarev ED, Maresz K, Tan Y, Dittel BN (2007) CNS-derived interleukin-4 is essential for the regulation of autoimmune inflammation and induces a state of alternative activation in microglial cells. *J Neurosci* **27**:10714–10721.
40. Rodriguez PC, Zea AH, DeSalvo J (2003) L-arginine consumption by macrophages modulates the expression of CD3 zeta chain in T lymphocytes. *J Immunol* **171**:1232–1239.
41. Rutschman R, Lang R, Hesse M, Ihle JN, Wynn TA, Murray PJ (2001) Cutting edge: Stat6-dependent substrate depletion regulates nitric oxide production. *J Immunol* **166**:2173–2177.
42. Segal BM (2010) Th17 cells in autoimmune demyelinating disease. *Semin Immunopathol* **32**:71–77.
43. Shechter R, London A, Varol C (2009) Infiltrating blood-derived macrophages are vital cells playing an anti-inflammatory role in recovery from spinal cord injury in mice. *Plos Med* **6**:e1000113.
44. Slaney CY, Toker A, La FA, Backstrom BT, Harper JL (2011) Naive blood monocytes suppress T-cell function. A possible mechanism for protection from autoimmunity. *Immunol Cell Biol* **89**:7–13.
45. Stuve O, Youssef S, Slavin AJ, King CL, Patarroyo JC, Hirschberg DL *et al* (2002) The role of the MHC class II transactivator in class II expression and antigen presentation by astrocytes and in susceptibility to central nervous system autoimmune disease. *J Immunol* **169**:6720–6732.
46. Suzuki M, Konya C, Goronzy JJ (2008) Inhibitory CD8+ T cells in autoimmune disease. *Hum Immunol* **69**:781–789.

© 2011 The Authors; Brain Pathology © 2011 International Society of Neuropathology

47. Takahashi K, Prinz M, Stagi M (2007) TREM2-transduced myeloid precursors mediate nervous tissue debris clearance and facilitate recovery in an animal model of multiple sclerosis. *Plos Med* **4**:e124.
48. Talmadge JE (2007) Pathways mediating the expansion and immunosuppressive activity of myeloid-derived suppressor cells and their relevance to cancer therapy. *Clin Cancer Res* **13**:5243–5248.
49. Varin A, Gordon S (2009) Alternative activation of macrophages: immune function and cellular biology. *Immunobiology* **214**:630–641.
50. Vignali DA, Collison LW, Workman CJ (2008) How regulatory T cells work. *Nat Rev Immunol* **8**:523–532.
51. Wu F, Cao W, Yang Y, Liu A (2010) Extensive infiltration of neutrophils in the acute phase of experimental autoimmune encephalomyelitis in C57BL/6 mice. *Histochem Cell Biol* **133**:313–322.
52. Xu L, Hilliard B, Carmody RJ (2003) Arginase and autoimmune inflammation in the central nervous system. *Immunology* **110**:141–148.
53. Youn JI, Gabrilovich DI (2010) The biology of myeloid-derived suppressor cells: the blessing and the curse of morphological and functional heterogeneity. *Eur J Immunol* **40**:2969–2975.
54. Zehntner SP, Brickman C, Bourbonniere L (2005) Neutrophils that infiltrate the central nervous system regulate T cell responses. *J Immunol* **174**:5124–5131.
55. Zhu B, Bando Y, Xiao S (2007) CD11b+Ly-6C(hi) suppressive monocytes in experimental autoimmune encephalomyelitis. *J Immunol* **179**:5228–5237.

SUPPORTING INFORMATION

Additional Supporting Information may be found in the online version of this article:

Figure S1. Spinal cords of sham mice showed no Arg-I expression at 15 dpi (clinical score: 0). A–I: Whereas no Gr-1 immunostaining was observed in the spinal cord of sham animals (A, C), $CD11b^+$- (D) and M-$CSF1R^+$-microglial cells (G) were detected. In all three cases, no Arg-I-immunoreactivity was detected (B, E–F, H–I). Scale bar: A–C, G–I = 40 μm; D–F = 50 μm.
Figure S2. Quantification of $Gr\text{-}1^+$-. $CD11b^+$- and M-$CSF1R^+$-cells at the time points at which Arg-I^+-cells were present. A–F: The density of each MDSC marker paralleled that of the Arg-I^+-cells (Gr-1: A; CD11b: C; M-CSF1R: F). However, the percentage of $Gr\text{-}1^+$- (B), $CD11b^+$- (D) or M-$CSF1R^+$-cells (F) displaying Arg-I immunoreactivity remained constant at both 15 dpi and 25 dpi. The results were analyzed with the Student's *t* test applying the critical value of $P < 0.001$ (***).

Please note: Wiley-Blackwell are not responsible for the content or functionality of any supporting materials supplied by the authors. Any queries (other than missing material) should be directed to the corresponding author for the article.

© 2011 The Authors; Brain Pathology © 2011 International Society of Neuropathology